5th International Symposium on Three-Dimensional Electromagnetics
Sapporo, Japan, May 7–9, 2013

Resolution of full waveform inversion using controlled-source electromagnetic exploration

Naoto Imamura[1], Tada-nori Goto[1], Junichi Takekawa[1] and Hitoshi Mikada[1]
[1]Kyoto University

SUMMARY

A 3D full waveform inversion method is presented using a controlled-source electromagnetic (CSEM) method. We demonstrate that conductive anomalies around subsurface could be estimated from data simulated for a synthetic model. We discuss the resolution of our CSEM inversion method, in terms of the distribution and the orientation of dipoles of transmitter and receivers. We considered two cases in the alignment of x-oriented receiver and transmitter dipole arrays: (i) 2D inline alignment of the arrays, and (ii) pseudo 3D parallel offset alignment. Our synthetic inversion examples show that the latter could lead to the resolution of results higher than the former, in particular deeper part of our subseafloor model. We then confirmed that the utilization of tricomponent transmitters and receivers could give better locations both in horizontal and vertical directions in inversion results than that of x-oriented dipoles only. These differences of the inversion results could be explained by the distribution of electric flux and charge around the boundary of conductive anomalies. We would like to conclude, from these results, that it would be essential to consider the deployment of multicomponent transmitter and receivers whose arrays are aligned in 3D for reliable inversion.

Keywords: marine CSEM, FDTD, full waveform inversion

INTRODUCTION

Controlled source electromagnetic (CSEM) method is widely used for shallow subsurface explorations to measure resistivity structure in detail. This method is also used for surveying oil and natural gas resources in deep sea. Recently, theoretical and experimental attempts have been initiated to survey submarine massive sulphides (SMS) using electromagnetic method. Kowalczyk (2008) surveyed SMS using EM method with magnetic source, although the sounding depth was limited within several meters. From conventional studies about SMS, some features of SMS become clear. Nakayama et al.(2011) found that core samples of SMS showed high IP effects. Imamura et al.(2011) showed that the thickness of SMS is proportional to the attenuated rate of amplitude of electromagnetic fields. Various kinds of inversion methods in frequency domain of electromagnetic method have been developed, although these methods require solutions for each frequency in the source spectrum. In this paper, we present the implementation of a full waveform inversion algorithm to simulate multi-frequencies at a time. For full waveform inversion method in CSEM, Zhdanov and Portniaguine (1997) derived basic theory of this inversion method and confirmed the effectiveness in their numerical study. Zhdanov et al. (2010) applied this inversion method to real field data.
In time-domain electromagnetic method, FDTD method is often used for forward calculation (de la Kethulle de Ryhove, 2012). The advantages of FDTD method is that it does not require the solution of systems of linear equations. Another advantages is that various kinds of frequencies can be computed from a single FDTD simulation. However, many previous researches showed that FDTD method with low frequency transmitter requires huge number of time steps. In this study, we solve the problem employing fictitious wave domain method (Mittet, 2010). In this method, electromagnetic fields are calculated in fictitious wave domain and transformed to diffusive domain employing mathematical transform. Time step in FDTD method becomes much larger than the time step derived from courant condition.
From previous researches, observed electromagnetic fields highly depend on the orientation of transmitter. Weiss and Constable (2006) discussed the influence of the orientation of transmitter/receiver to Fréchet sensitivity kernels. We discussed our results in terms of resolution of inversion results, considering distribution and orientations of transmitter/receiver. We also integrated results of different oriented dipoles. As a result, it is found that the array distribution and orientation of transmitter/receiver are keys to determine resolution of inversion results.

METHOD

It is very time consuming to simulate with low frequency transmitter, because of huge numbers of time steps. In order to calculate FDTD method with large time steps such as real field data, fictitious wave domain method developed by Mittet (2010) is employed. Frequency domain

Maxwell equations are transformed to fictitious wave domain employing a following equation,

$$\omega' = (i+1)\sqrt{\omega\omega_0} \quad (1)$$

where ω_0 is a scale parameter, ω is angular frequency. Employing this equation, fictitious wave domain Maxwell equations in time domain are derived as follows,

$$-\nabla \times \mathbf{H}'(\mathbf{x},t') + \epsilon'(\mathbf{x})\frac{\partial}{\partial t'}\mathbf{E}'(\mathbf{x},t') = -\mathbf{J}'(\mathbf{x},t'), \quad (2)$$

$$\nabla \times \mathbf{E}'(\mathbf{x},t') + \mu\frac{\partial}{\partial t'}\mathbf{H}'(\mathbf{x},t') = -\mathbf{K}'(\mathbf{x},t') \quad (3)$$

where ϵ' satisfies $\epsilon'(\mathbf{x}) = \sigma(\mathbf{x})/2\omega_0$, **E**' and **H**' are electromagnetic fields in the fictitious wave domain and **J**' and **K**' are electromagnetic sources in the fictitious wave domain. Depending on the value of ω_0, velocity of electromagnetic fields can be set optimally. In this study, we set ω_0 as 6.28. When ω_0 equals to 6.28 and grid size equals to 20 m, the maximum time step length becomes to 0.001977 s. This value is much larger than a time step length based on courant condition.
In our full waveform inversion method, model conductivity in the next iteration is calculated based on,

$$\sigma_{n+1} = \sigma_n + \alpha_n \mathbf{W}_n^{-1} \sum_{trn} \int_\Omega \mathbf{E}(x,\omega)\cdot\mathbf{E}_b(x,\omega|\delta\mathbf{E})d\omega \quad (4)$$

where $\mathbf{E}_b$ is a backpropagted electric fields, $\delta\mathbf{E}$ is a difference between observed electric fields and simulated electric fields and $\mathbf{W}_n$ is a weighting function derived from sensitivity. In this study, $\mathbf{E}_b$, $\delta\mathbf{E}$ and $\mathbf{W}_n$ are calculated from

$$\mathbf{E}_b(x,\omega|\delta\mathbf{E}) = \int\int_S \mathbf{G}^{EJ}(x,\omega;x_r)\cdot\delta\mathbf{E}(x_r,\omega)ds \quad (5)$$

$$\delta\mathbf{E}(x_r,\omega|x_s) = \mathbf{E}(x_r,\omega;x_s)_{obs} - \mathbf{E}(x_r,\omega;x_s)_{cal} \quad (6)$$

$$\mathbf{W}_n = \sqrt{\int_\Omega\int\int_\Sigma |\mathbf{G}^{EJ}(x|x')\cdot\mathbf{E}(x')|^2 ds d\omega} \quad (7)$$

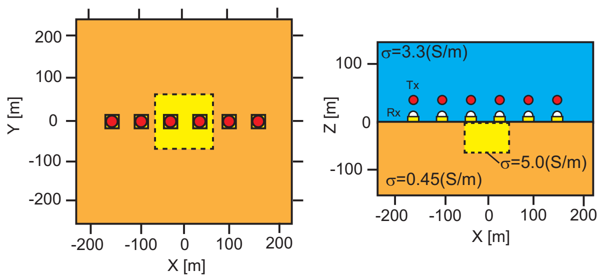

Figure 1. The synthetic model with a 2D alignment of transmitter and receivers consisting of conductive anomaly, seawater and resistive basement.

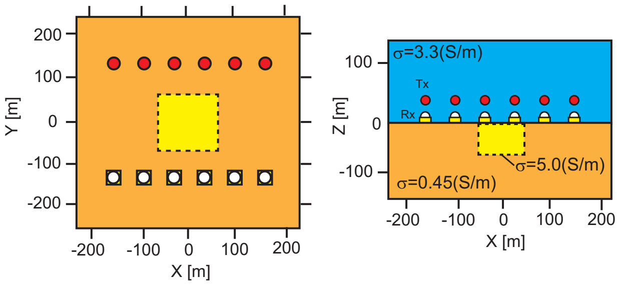

Figure 2. The synthetic model with a 3D alignment of transmitter and receivers consisting of conductive anomaly, seawater and resistive basement.

Each green functions are calculated from FDTD simulation. We use X-component of transmitted electric current and X-component of received electric field to calculate model gradient. Step length of model gradient is determined by parabolic optimization (Vigh et al., 2009). For absorbing boundary layer, the convolutional prefectly matched layer (CPML) is employed for five grids.

RESULTS AND DISCUSSION

In this study, we set the synthetic models as Figure 1 and Figure 2 assuming the SMS. In Figure 1, the distribution of transmitter and receivers are 2D arrangement In Figure 2, the distribution of transmitter and receivers are 3D arrangement. A transmitter and six receivers are arranged above the anomaly. Electric current is transmitted while the transmitter moves to six positions. We set a transmitted waveform as ricker wavelet with a center frequency of 1 Hz. The dipole is set to 1 m length and 1 A. We used 20 numbers of frequencies from 0 Hz to 7.3 Hz. We also set the grid size as 20m and the number of grid is 31 in each direction. The initial model is set as a two-layer model.
Inversion results in the plane of Y = 0 m are shown in Figure 3. In each figure, a rectangle shows the existence of conductive anomaly. In Figure 3(a) and (b), we set the orientations of transmitter as x-direction. In Figure 3(c), we consider three-components of transmitter and receivers simultaneously. As shown in Figure 3, the resolution of the inversion results is different. In case of Figure 3(a), the horizontal position of the conductive anomaly is detected. Figure 3(a) also shows that the inversion result has low resolution for deeper area of conductive anomaly in case of 2D distributed array. Figure 3(b) shows that the inversion result has high resolution for horizontal and vertical position in case of 3D distributed array. Figure 3(c) shows that the inversion result has high resolution comparing with Figure 3(a) and (b). These differences of the inversion results are explained considering distribution of electric flux and electric charge around the boundary of the conductive anomaly. In case of 2D distributed array, horizontal component of electric field is dominant beneath the anomaly. Because of this, the amount of electric charge

beneath the anomaly is low. In case of 3D distributed array, vertical component of electric field is dominant comparing with 2D results. This is because the vertical position of anomaly is resolved precisely in case of Figure 3(b) and (c).

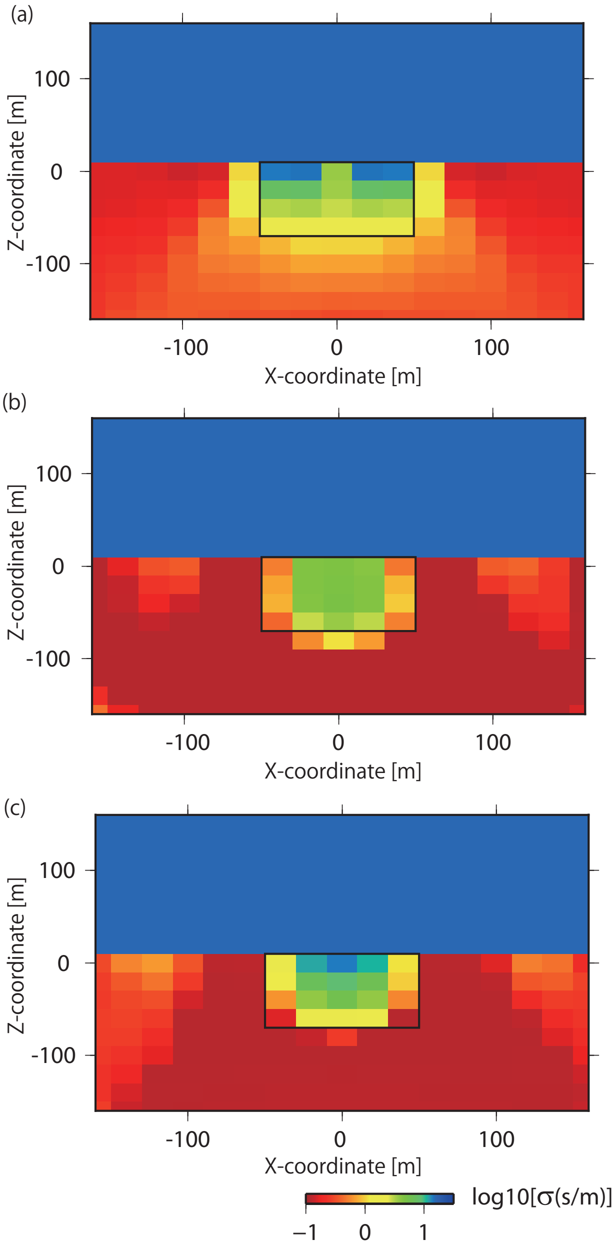

Figure 3. Comparison of inversion results changing the distribution and the orientation of transmitter and receivers. (a) The transmitter and receivers are distributed as 2D array. (b) The transmitter and receivers are distributed as 3D array. (c) The transmitter and receivers are distributed as 3D array and oriented to 3-components.

CONCLUSION

A full waveform CSEM inversion with the fictitious wave domain method was developed and implemented for a synthetic model. We compared the effect of distribution of dipoles, and discussed resolution of inversion results with conductive anomaly. From the results, we found that the resolution depends on the distribution of transmitter and receivers. We integrated inversion results of different oriented dipoles. As a result, the resolution of deeper area is improved with 3D distributed array of dipoles. The resolution of anomaly is also improved when three components of transmitter are employed. Through all numerical results, we conclude that it is important to consider optimum distribution of dipoles and orientation of dipoles for effective inversion.

ACKNOWLEDGMENTS

We are greatly thankful to the financial support of SMS exploration project by Ministry of Education, Culture, Sports, Science and Technology in Japan. We are also grateful to the Japan Society for the Promotion of Science (JSPS 24·372) for the Grants-in-Aid for Science Research in the Research Fellowship program that supported the present study.

REFERENCES

de la Kethulle de Ryhove, S. (2012). 3D finite-difference time-domain marine magnetotelluric modelling . *Extended Abstracts, 21th EMIW*.

Imamura, N., Goto, T., Takekawa, J., & Mikada, H. (2011). Application of Marine Controlled-source Electromagnetic Sounding to Submarine Massive Sulphides Explorations. *SEG Technical Program Expanded Abstracts 2011*, 730–734.

Kowalczyk, P. (2008). Geophysical prelude to first exploitation of submarine massive sulphides. *First Break*, *26*(11), 99–106.

Mittet, R. (2010). High-order finite-difference simulations of marine CSEM surveys using a correspondence principle for wave and diffusion fields. *Geophysics*, *75*(1), F33.

Nakayama, K., Shingyouji, T., & Motoori, M. (2011). Marine Time-domain electromagnetic technologies for the ocean bottom mineral resources. In *Proceedings of the 10th segj international symposium* (pp. 433–436).

Vigh, D., Starr, E. W., & Kapoor, J. (2009). Developing Earth models with full waveform inversion. *The Leading Edge*, *28*(4), 432–435.

Weiss, C. J., & Constable, S. (2006). Mapping thin resistors and hydrocarbons with marine EM methods, Part II — Modeling and analysis in 3D. *Geophysics*, *71*(6), G321.

Zhdanov, M. S., & Portniaguine, O. (1997). Time-domain electromagnetic migration in the solution of inverse problems. *Geophysical Journal International*, *131*(2), 293–309.

Zhdanov, M. S., Velikhov, E. P., Cuma, M., Wilson, G., Black, N., & Gribenko, A. (2010). Exploring multiple 3D inversion scenarios for enhanced interpretation of marine CSEM data: An iterative migration analysis of the Shtokman gas field: Barents Sea. *First Break*, *28*(3), 95–101.